Electronic Supplementary Information

Experimental details

Materials characterization. Powder X-ray diffraction (XRD) tests were carried out on a Bruker D8 Advance X-ray instrument (Cu $K_{\alpha 1}$ radiation, λ= 1.5406 Å) at a voltage of 40 kV and a current of 40 mA. Field-emission scanning electron microscope (FESEM; Helios G4 CX) and transmission electron microscope (TEM; JEOL, JEM-2010) were used to examine the morphology and structure of the samples. The compositions of the samples were determined by energy-dispersive X-ray spectroscopy (EDX) attached to scanning electron microscope (SEM; Quanta 250) and inductively coupled plasma emission spectrometer (iCAP7400). X-ray photoelectron spectroscopy (XPS) analysis and Ultraviolet photoelectron spectra were carried out on a PHI Quantum 2000 XPS system with C 1s binding energy (284.6eV) as the reference and He I excitation (21.22 eV) as the monochromatic light source. N_2 and CO_2 adsorption–desorption isotherms characterizations were conducted on a Micromeritics ASAP2020 under liquid nitrogen temperature (77 K) and under mixture of ice and water (273K). UV-vis diffuse reflectance spectra (DRS) were obtained using a Varian Cary 500 UV-vis spectrometer equipped with an integrating sphere, and $BaSO_4$ was used as a reference. The room temperature photoluminescence (PL) characterizations were carried out on Hitachi F-7000 spectrophotometer. The fluorescence lifetime is determined by recording the time-resolved fluorescence emission spectra on a Deltapro Fluorescence Lifetime System. A Nicolet IS50 FTIR spectrometer (Thermo SCIENTIFIC) was employed to collect the Fourier transform infrared (FTIR) spectra. The electrochemical analysis carried out on Metrohm Autolab Electrochemical System, using a conventional three electrodes cell with Pt electrode and Ag/AgCl electrode as the counter electrode and reference electrode, respectively. Typically, 5 mg of the sample was dispersed in N, N-dimethylformamide (1 mL) by sonication to gain a

slurry. Then, the resultant slurry was spread onto the FTO glass with an area of ca. 0.25 cm^2. The transient photocurrent response spectra were collected in Na_2SO_4 aqueous solution (0.2 M) with a 300 W xenon lamp ($\lambda \geq 420$ nm) as a light source. Electrochemical impedance spectroscopy (EIS) measurements were carried out at the open circuit potential. In situ electron spin resonance (ESR) measurement was then carried out on a Bruker A300 under liquid nitrogen temperature. Absorption spectra were obtained on a UV-vis spectrophotometer (HITACHI UH5300). The ESR tests were performed at liquid nitrogen temperature. A certain amount of ZnS-DETA/CdS, $Co(bpy)_3^{2+}$, and mixed solution of H_2O/ acetonitrile/TEOA were transferred into the ESR test tube, which was then bubbled with CO_2 for 5 min and sealed. A 300 W xenon lamp ($\lambda \geq 420$ nm) was used as the light source. The UV-vis absorption experiments were conducted at room temperature. Typically, 4 mg of photocatalyst, 8 μmol of $CoCl_2$, 400 μmol of 2'2-bipyridine (bpy), 16 mL of acetonitrile, 4 mL of H_2O, and 4 mL of TEOA were added into a glass beaker to get a uniform suspension. Then, 3 mL of the suspension was transferred into the quartz cuvette. The suspension in quartz cuvette was bubbled with CO_2 for 10 min and sealed. A 300 W xenon lamp ($\lambda \geq 420$ nm) was used as the light source.

The produced gases after photocatalytic CO_2 reduction reactions were analyzed and quantified by an Agilent 7890B gas chromatography (GC). The H_2 gas was analyzed and quantified by the GC equipped with a thermal conductivity detector (TCD) and a TDX-1 packed column. The CO product was converted to CH_4 by a methanizer and then analyzed by a flame ionization detector (FID). Ar was used as the carrier gas. A HP5973 gas chromatography-mass spectrometry (GC-MS) was employed to detect the ^{13}CO generated from the $^{13}CO_2$ isotopic experiment.

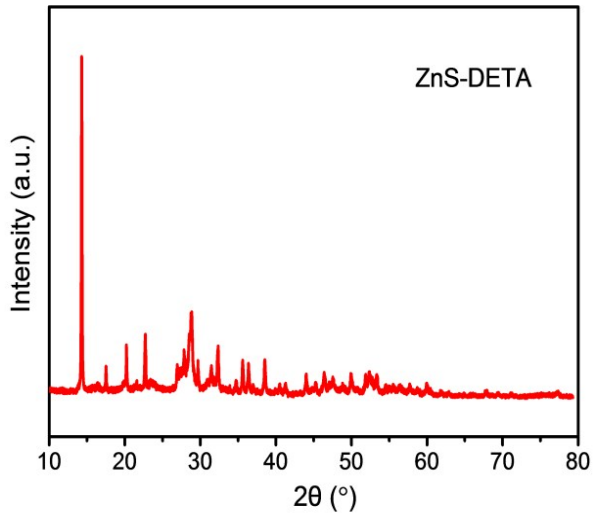

Fig. S1 XRD pattern of ZnS-DETA hybrid nanosheets.

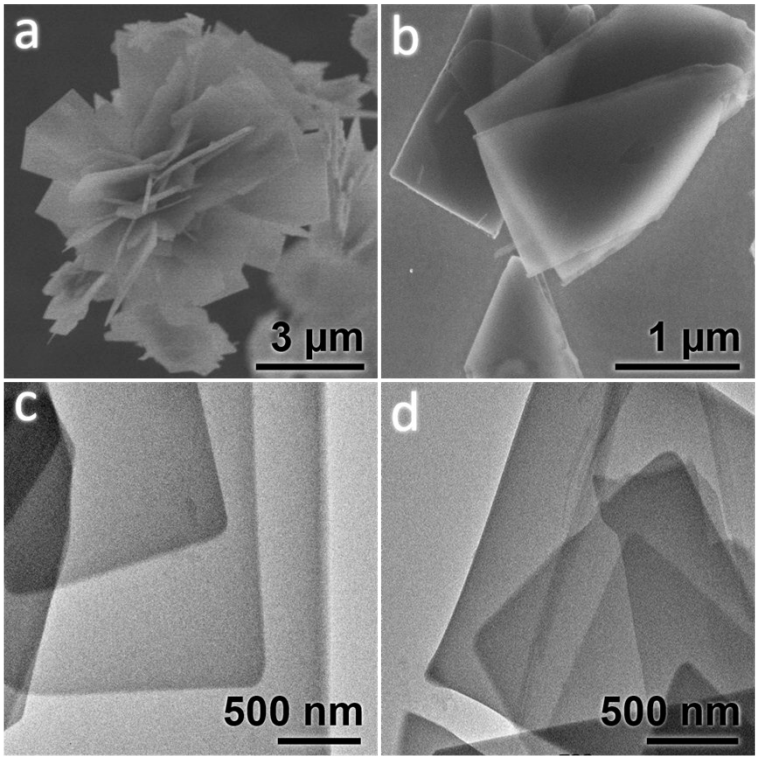

Fig. S2 (a,b) FESEM images and (c,d) TEM images of ZnS-DETA nanosheets.

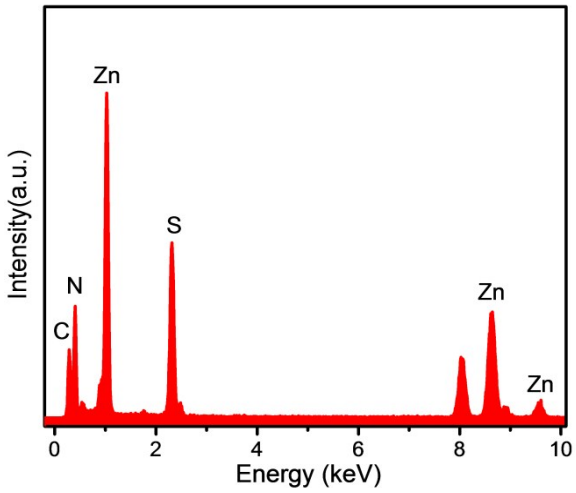

Fig. S3 EDX spectrum of ZnS-DETA hybrid nanosheets.

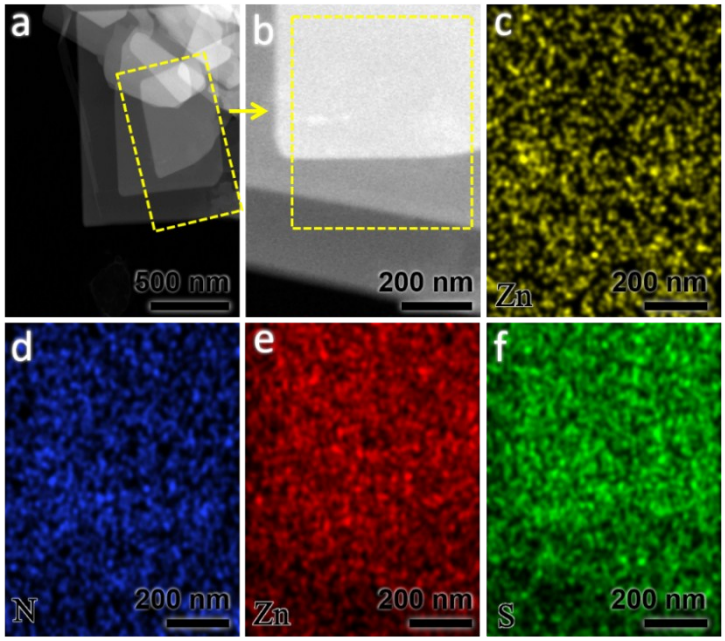

Fig. S4 (a,b) TEM images and (c-f) elemental mapping images of ZnS-DETA hybrid nanosheets.

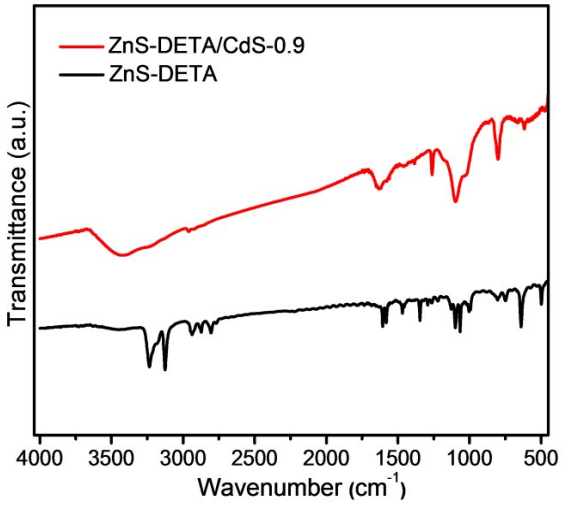

Fig. S5 FTIR spectra of ZnS-DETA and ZnS-DETA/CdS.

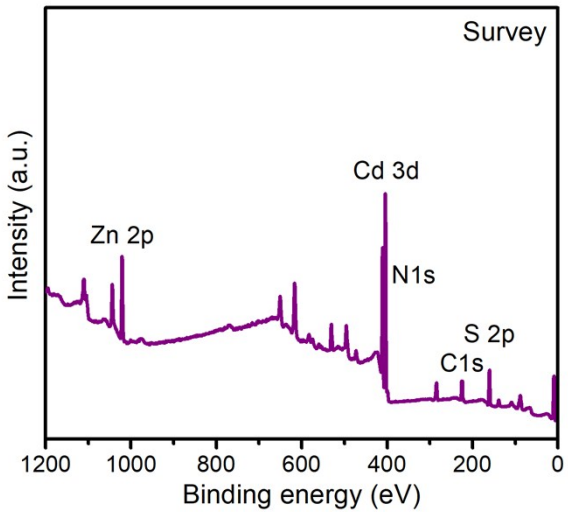

Fig. S6 Survey XPS spectrum of ZnS-DETA/CdS.

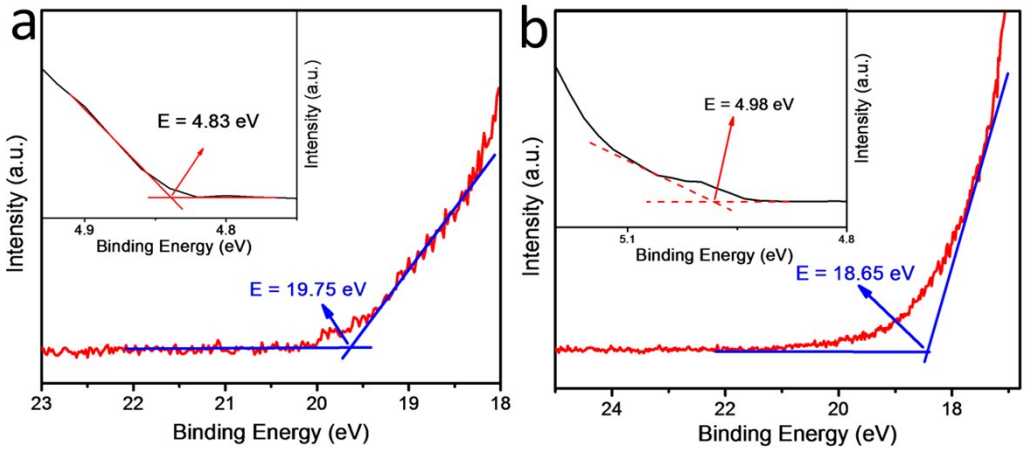

Fig. S7 UPS spectra of (a) CdS and (b) ZnS-DETA. The inset shows the onset values for the valence band.

A complete description of the calculation process of the valence band maximum and the minimum of the conduction band from UPS spectra.

The work function (φ) can be calculated using Eq. (1): $\varphi = hv - E_{SEO}$. Here, hv = 21.22 eV, represents the energy of the monochromatic ionizing light, while E_{SEO} is the secondary electron onset, obtained from the linear extrapolation of the UPS spectrum.

The Fermi level (E_F) is obtained from the work function using Eq. (2): $E_F = -\varphi$.

The position of the valence band maximum (E_{VB}) is obtained from Eq. (3): $E_{VB} = E_F - X$, in which X is obtained from the extrapolation of the onsets in the UPS spectrum.

The conduction band minimum potential (E_{CB}) is obtained from Eq. (4): $E_{CB} = E_{VB} + E_{BG} = E_F - X + E_{BG}$. Here, the bandgap energy E_{BG} is obtained by Tauc plots.

The conduction band (CB) positions of CdS and ZnS-DETA are determined by the UPS spectra. The work function of CdS was estimated to be 1.47 eV, applying the method of a linear approximation to the UPS spectra. The Fermi level of CdS was estimated to be -1.47 eV. Simultaneously, the valence band maximum was calculated to be -6.30 eV. The average band gap energy value (2.49 eV for CdS) obtained from the Tauc plots (Figure 6b). The minimum of the conduction

band is located at -3.90 eV. The calculated potentials refer to the vacuum level (E_{Vac}). Therefore, according to the relationship between the potential of the reversible hydrogen electrode (RHE) and E_{Vac} (i.e., $E_{RHE} = -E_{Vac} - 4.44$), the conduction and valence band of CdS are determined to be -0.63 and 1.86 V vs. RHE, respectively. The value of the potential of RHE equals to the normal hydrogen electrode (NHE) at pH = 0. The conduction and valence band of CdS are located at -1.04 and 1.45 V (vs. NHE, pH=7), respectively. Similarly, the valence band maximum and the minimum of the conduction band of ZnS-DETA are 2.74 and -0.70 V (vs. NHE, pH=7), respectively.

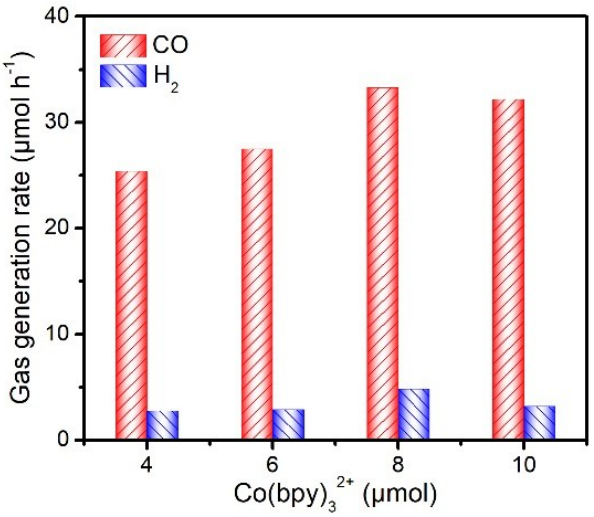

Fig. S8 Photocatalytic CO_2 reduction performance of ZnS-DETA/CdS with different amounts of $Co(bpy)_3^{2+}$ (Co^{2+}/bpy = 1:50) added in the reaction system. Reaction conditions: ZnS-DETA/CdS (4 mg), TEOA (4 ml), acetonitrile (16 ml), H_2O (4 ml), CO_2 (1 atm), and visible light irradiation ($\lambda \geq 420$ nm).

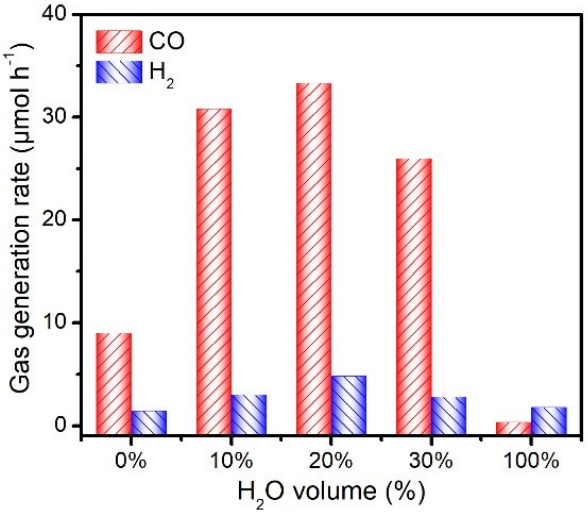

Fig. S9 Photocatalytic CO_2 reduction performance of ZnS-DETA/CdS in the reaction systems with different volumetric ratios of H_2O in the mixture solvent of H_2O/MeCN.

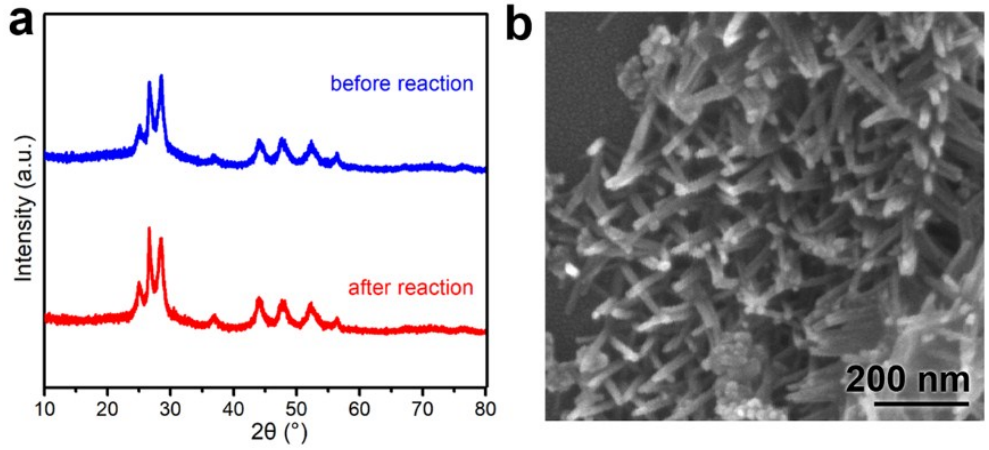

Fig. S10 (a) XRD patterns of fresh and used ZnS-DETA/CdS sample and (b) FESEM image of used ZnS-DETA/CdS sample.

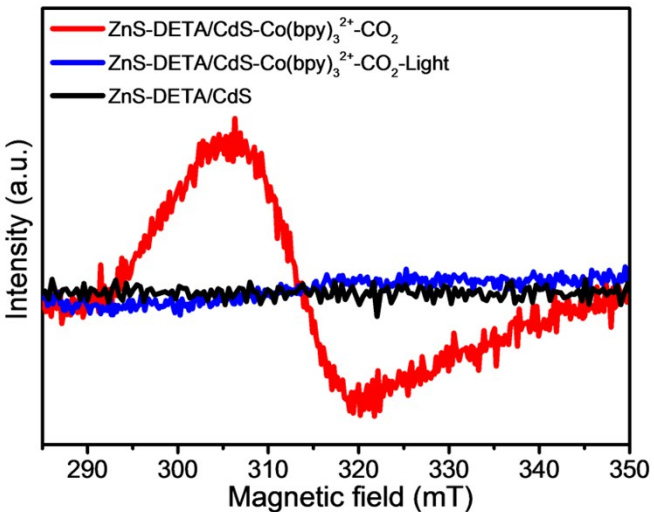

Fig. S11 ESR spectra of the photocatalytic CO_2 reduction systems under different conditions.

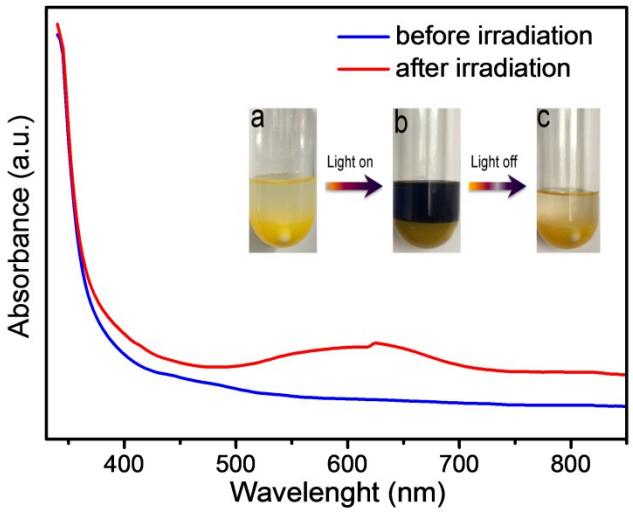

Fig. S12 UV-vis absorption spectra of the photocatalytic CO_2 reduction systems before and after visible light irradiation. Insets are the corresponding photographs: (a) the fresh reaction mixture, (b) upon visible light irradiation and (c) after the reaction light.

Table S1. Molar ratios of Zn/Cd of different samples determined by ICP-OES.

Sample	Zn/Cd
ZnS-DETA/CdS-0.50	1: 2.34
ZnS-DETA/CdS-0.85	1: 2.55
ZnS-DETA/CdS-0.90	1: 2.58
ZnS-DETA/CdS-0.95	1: 2.63

Table S2. Comparison of CO generation rate of ZnS-DETA/CdS with those of other catalysts in similar CO_2 photoreduction systems using $Co(bpy)_3^{2+}$ as a cocatalyst.

Catalyst (used amount)	Cocatalyst	Sacrificial agent	CO evolution rate [a] (μmol h^{-1})	Ref.
ZnS-DETA/CdS (4 mg)	$Co(bpy)_3^{2+}$	TEOA	CO: 33.3	This work
CdS/BCN (50mg)	$Co(bpy)_3^{2+}$	TEOA	CO: 12.5	1
CdS/ZIF-8 (40 mg)	$Co(bpy)_3^{2+}$	TEOA	CO: 32.1	2
Au(25)@CdS (4 mg)	$Co(bpy)_3^{2+}$	TEOA	CO: 15	3
PCN/$ZnIn_2S_4$ (50mg)	$Co(bpy)_3^{2+}$	TEOA	CO: 44.6	4
$ZnIn_2S_4$-In_2O_3 (4mg)	$Co(bpy)_3^{2+}$	TEOA	CO: 12.3	5
CNU-BA0.03 (30 mg)	$Co(bpy)_3^{2+}$	TEOA	CO: 31.1	6
2D TiO-CN (3 mg)	$Co(bpy)_3^{2+}$	TEOA	CO: 0.85	7
In_2S_3-$CdIn_2S_4$ (4mg)	$Co(bpy)_3^{2+}$	TEOA	CO: 3.3	8
DA-CTF (30 mg)	$Co(bpy)_3^{2+}$	TEOA	CO: 4	9
Co_4@g-C_3N_4 (50 mg)	$Co(bpy)_3^{2+}$	TEOA	CO: 5.4	10

[a] The CO evolution rate is calculated based on the used amount of catalyst in the reaction system.

Supplementary References

1. M. Zhou, S. Wang, P. Yang, C. Huang and X. Wang, *ACS Catal.*, 2018, **8**, 4928-4936.
2. Y. Liu, L. Deng, J. Sheng, F. Tang, K. Zeng, L. Wang, K. Liang, H. Hu and Y.-N. Liu, *Appl. Surface Sci.*, 2019, **498**, 143899.
3. P. Zhang, S. Wang, B. Y. Guan and X. W. Lou, *Energy Environ. Sci.*, 2019, **12**, 164-168.
4. M. Zhou, S. Wang, P. Yang, Z. Luo, R. Yuan, A. M. Asiri, M. Wakeel and X. Wang, *Chem. Eur. J.*, 2018, **24**, 18529-18534.
5. S. Wang, B. Y. Guan and X. W. Lou, *J. Am. Chem. Soc.*, 2018, **140**, 5037-5040.
6. J. Qin, S. Wang, H. Ren, Y. Hou and X. Wang, *Appl. Catal. B Environ.*, 2015, **179**, 1-8.
7. S. Tang, X. Yin, G. Wang, X. Lu and T. Lu, *Nano Res.*, 2018, **12**, 457-462.
8. S. Wang, B. Y. Guan, Y. Lu and X. W. Lou, *J. Am. Chem. Soc.*, 2017, **139**, 17305-17308.

9. H. Zhong, Z. Hong, C. Yang, L. Li, Y. Xu, X. Wang and R. Wang, *ChemSusChem*, 2019, **12**, 4493-4499.
10. J. Zhou, W. Chen, C. Sun, L. Han, C. Qin, M. Chen, X. Wang, E. Wang and Z. Su, *ACS Appl. Mater. Interfaces*, 2017, **9**, 11689-11695.